Mathematical modeling of short and ultrashort laser action on metals

V.I. Mazhukin*, A.V.Mazhukin, M.M.Demin, A.V.Shapranov
Keldysh Institute of Applied Mathematics,
Miusskaya pl. 4A,
125047 Moscow, Russia.
*Corresponding author: vim@modhef.ru

Abstract

Short pulsed laser action on aluminum is considered. Pulsed nano- and picoseconds action is characterized by non-equilibrium heating of metals described within the framework of two-temperature approximation. Rapid heating is caused by the appearance of phase transitions of the first order which velocity increases as the pulse duration drops and intensity rises. Mathematical modeling with explicit interphase front tracking allowed determining that fast phase transformations cause high degree of non-equilibrium of the processes which manifests itself as highly overheated metastable regions in solid and liquid phases.

The magnitude of overheating depends on the pulse duration. Typical overheating is tens and hundreds of degrees in the nanosecond range and thousands of degrees in the picoseconds range.

1. Introduction

Pulsed laser ablation is widely used for surface modification and material nanostructuring [1]. However, consistent fundamental theory of pulsed laser ablation in wide rage of the pulse frequency and duration is far from its completion. The main ablation mechanisms and their interchange are still unclear in spite of impressive progress of theoretical works during recent 10 years [1] - [3] mostly based on molecular dynamic approach. High degree of non-equilibrium of the processes of laser heating with ultrashort pulses and corresponding dynamics of fast phase transitions make it difficult to determine the dominating ablation mechanisms and their interchange as the pulse duration and energy density change. In particular, all transport characteristics in the used models are highly non-equilibrium and are not known in the wide temperature and frequency range. These problems continue to stimulate further investigation of pulsed laser ablation.

The aim of this work is detailed investigation of the dynamics of laser ablation based on numerical solution of theoretical model describing short (nanosecond) and ultrashort (picosecond) high-power laser action on metals within the approximation of Stephan type non-equilibrium hydrodynamic model with explicit front tracking.

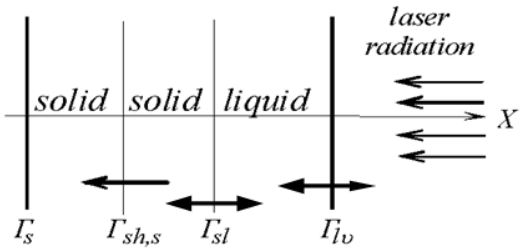

Fig.1: Spatial phase configuration

2. Theoretical model

Laser radiation propagates from the right to the left and is partially absorbed at the surface of the metal target. Fig.1 shows spatial configuration of the phase fronts $\Gamma_{sl}(t), \Gamma_{lv}(t)$ and the shock wave in the condensed media $\Gamma_{sh,s}(t)$. The statement of the problem includes the following limitations and suppositions.

The mechanisms of volume melting and evaporation are not included in consideration. It is supposed that the melting front appear at the irradiated surface when the temperature reaches T_{m0} and overheated metastable states behave in a stable way during consideration.

Mathematical description and modeling of femtosecond laser ablation of hard Aluminum target in vacuum is performed within the framework of non-equilibrium Stephan-type hydrodynamic and two-temperature and spatially one-dimensional model with multiple fronts written for two media: solid and liquid.

$$\left(\begin{array}{l}
\dfrac{\partial\rho}{\partial t}+\dfrac{\partial(\rho u)}{\partial x}=0 \\
\dfrac{\partial(\rho u)}{\partial t}+\dfrac{\partial(\rho u^2)}{\partial x}+\dfrac{\partial P}{\partial x}=0 \\
\dfrac{\partial(\rho_e\varepsilon_e)}{\partial t}+\dfrac{\partial(\rho_e u\varepsilon_e)}{\partial x}=-\left(P\dfrac{\partial u}{\partial x}+\dfrac{\partial W_e}{\partial x}+g(T_e)(T_e-T_{ph})+\dfrac{\partial G}{\partial x}\right) \\
\dfrac{\partial(\rho\varepsilon_{ph})}{\partial t}=-\left(P\dfrac{\partial u}{\partial x}+\dfrac{\partial W_{ph}}{\partial x}-g(T_e)(T_e-T_{ph})\right) \\
\dfrac{\partial G}{\partial x}+\alpha(T_e)G=0, \qquad \rho_e=z\dfrac{m}{M}\rho, \\
P=P_e(\rho_e,T_e)+P_{ph}(\rho_{ph},T_{ph}), \quad \varepsilon_e=C_{ve}(T_e)T_e, \quad \varepsilon_{ph}=C_{vph}(T_{ph})T_{ph}
\end{array}\right)_k ,$$

$$t>0, \quad 0<x<\Gamma_{sl}\bigcup\Gamma_{sl}<x<\Gamma_{lv}$$

$$W_e=-\lambda(T_e,T_{ph})\frac{\partial T_e}{\partial x}, \qquad W_{ph}=-\lambda(T_{ph})\frac{\partial T_{ph}}{\partial x}, \qquad P(\rho,T)=P(\rho_e,T_e)+P(\rho_{ph},T_{ph}),$$

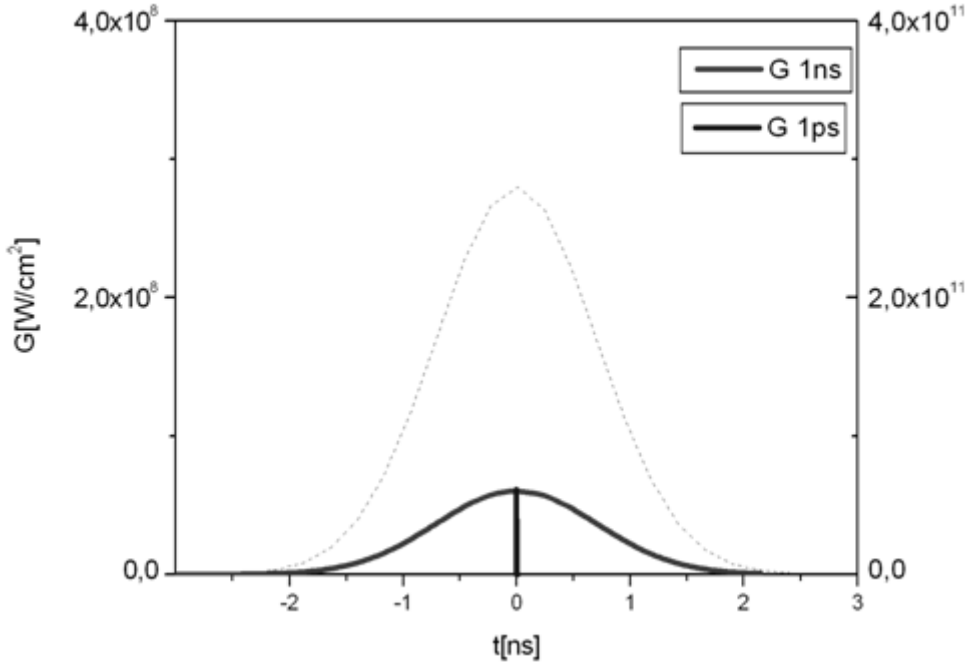

Fig.2: Time profile of nano- and picosecond pulses

Here: ρ, u, ε, T, P - are density, gas-dynamic velocity, internal energy and pressure, $\alpha(T_e), R(T_e)$ - are the coefficient of volume absorption and surface reflectivity, G is the laser radiation density, C_g λ - are the heat capacity and heat conductivity coefficient, $g(T_e)$ is the electron-phonon coupling constant. Indexes s, l, υ represent solid, liquid and vapor phases, e, ph represent electron and phonon gas, $k = s, l$

The model of surface non-equilibrium melting is represented by the following relations at

$$x = \Gamma_{sl}(t):\ \left(\lambda_e \frac{\partial T_e}{\partial x}\right)_s = \left(\lambda_e \frac{\partial T_e}{\partial x}\right)_\ell, \qquad T_{e,s} = T_{e,\ell},$$

$$\left(\lambda_{ph} \frac{\partial T_{ph}}{\partial x}\right)_s - \left(\lambda_{ph} \frac{\partial T_{ph}}{\partial x}\right)_\ell = \rho_s L_m^{ne} \upsilon_{s\ell}, \qquad \upsilon_{s\ell}(T_{s\ell}) = C T_{s\ell}^{1/2}\left[1 - \exp\left(\frac{L_m^{ne}}{RT_m}\frac{\Delta T_{s\ell}}{T_{s\ell}}\right)\right],$$

$$T_m = T_m(P_s) = T_{m,0} + kP_s, \qquad L_m^{ne} = L_m + \Delta C_{ps\ell}\Delta T_{s\ell} + \frac{\rho_s + \rho_\ell}{\rho_s - \rho_\ell}\frac{(u_s - u_\ell)^2}{2}.$$

$$\Delta C_{ps\ell} = (C_{p\ell} - C_{ps}), \qquad \Delta T_{s\ell} = (T_{s\ell} - T_m), \quad C = \alpha f_0 (2k_B / M)^{1/2} / \lambda .$$

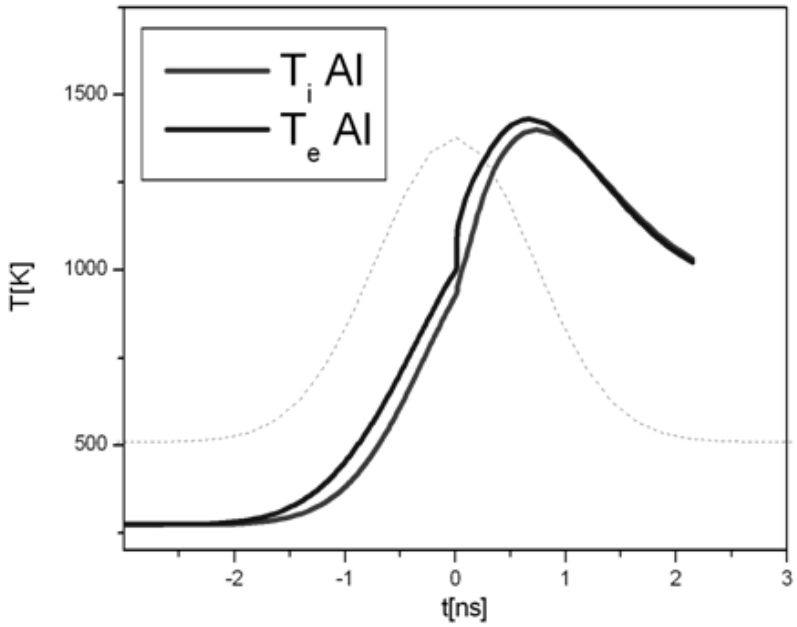

Fig. 3: Time dependence of electron and phonon temperature for τ=1ns

Surface evaporation is described within the approximation of non-equilibrium Knudsen layer:

$$x=\Gamma_{k\upsilon}(t):\ -\lambda_e\frac{\partial T_e}{\partial x}=\sigma T_e^4,\quad \left(\lambda_{ph}\frac{\partial T_{ph}}{\partial x}\right)_k-\left(\lambda_\upsilon\frac{\partial T_\upsilon}{\partial x}\right)_\upsilon=\rho_k L_\upsilon \upsilon_{k\upsilon},$$

$$\rho_k\upsilon_{k\upsilon}=\rho_\upsilon(\upsilon_{k\upsilon}-u),\qquad P_k+\rho_k\upsilon_{k\upsilon}^2=p_\upsilon+\rho_\upsilon(k\upsilon_\upsilon-u)^2,$$

$$\rho_\upsilon=\alpha_\rho(M)\rho_H,\ T_\upsilon=\alpha_T(M)T_{ph,k},\qquad P_H(T_{ph,k})=P_b\exp\left[\frac{L_\upsilon^{ne}}{RT_b}\left(\frac{\Delta T_{ph,k}}{T_{ph,k}}\right)\right],$$

$$\rho_H=\frac{P_H(T_{ph,k})}{RT_{phk}},\ L_\upsilon^{ne}=L_\upsilon^e(T_\ell)+C_{p\upsilon}(T_\upsilon-T_{ph,k})+\frac{\rho_\ell+\rho_\upsilon}{\rho_\ell-\rho_\upsilon}\frac{(u_\ell-u_\upsilon)^2}{2},$$

$$\rho_H=\frac{P_H(T_{ph,k})}{RT_{phk}},\ L_\upsilon^{ne}=L_\upsilon^e(T_\ell)+C_{p\upsilon}(T_\upsilon-T_{ph,k})+\frac{\rho_\ell+\rho_\upsilon}{\rho_\ell-\rho_\upsilon}\frac{(u_\ell-u_\upsilon)^2}{2},$$

$$\Delta T_{ph,k}=T_{ph,k}-T_b,\qquad G(t)=(1-R(T_e))\cdot G_0\exp\left(-\left(\frac{t}{\tau_L}\right)^2\right).$$

where $\upsilon_{k\upsilon},\upsilon_{s\ell}$ - velocity of evaporation and melting, L_υ^{ne},L_m^{ne}, - non-equilibrium energy of evaporation and melting, $\alpha_\rho(M)$, $\alpha_T(M)$, - Crout coefficients [4], P_b, T_m,T_b, - equilibrium evaporation pressure and temperature and melting temperature, T_υ, ρ_υ - temperature and density of vapor, ρ_{sat}, P_{sat} - density and pressure of evaporated vapor, σ - Stephan-Boltzmann constant.

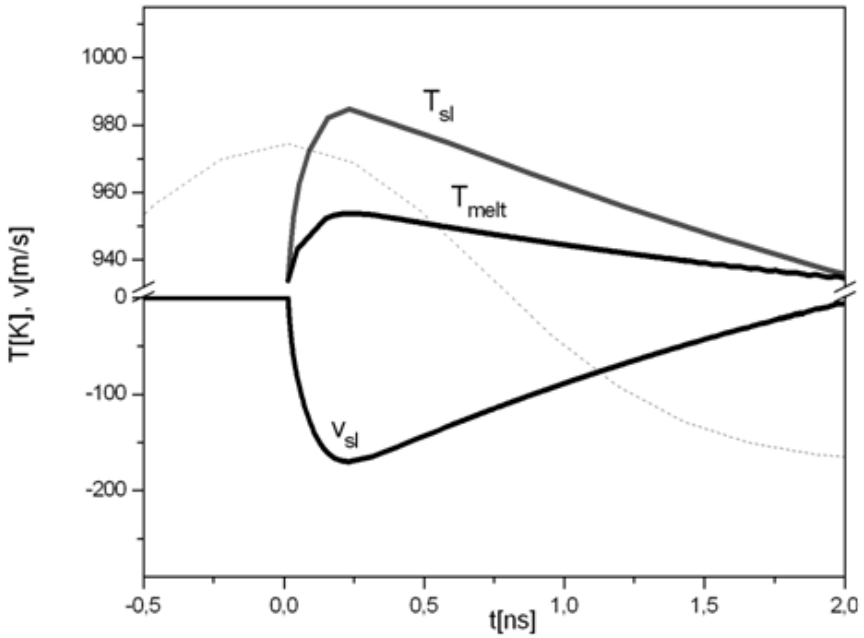

Fig. 4: Time dependence of the melting border temperature $T_{sl}(t)$, equilibrium melting temperature $T_m(P_s)$ and melting front velocity $v_{sl}(t)$ for $\tau=1ns$

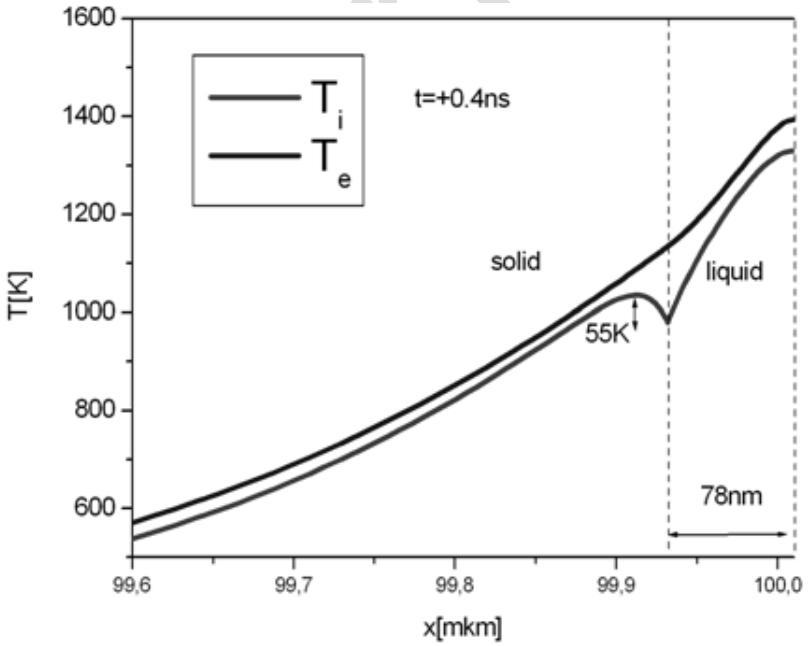

Fig. 5: Spatial profiles of T_e and T_{ph} for $\tau=1ns$

3. Modeling results

We consider two modes of pulsed laser action: short mode with $\tau_L=10^{-9}$ and ultra-short mode with $\tau_L=10^{-12}$ with Aluminum target with the same fluence $J=0.5J/cm^2$ and wavelength $\lambda_L=0.8$ μm. Fig. 2 shows time profile of incident and absorbed laser radiation for nano- and picosecond duration.

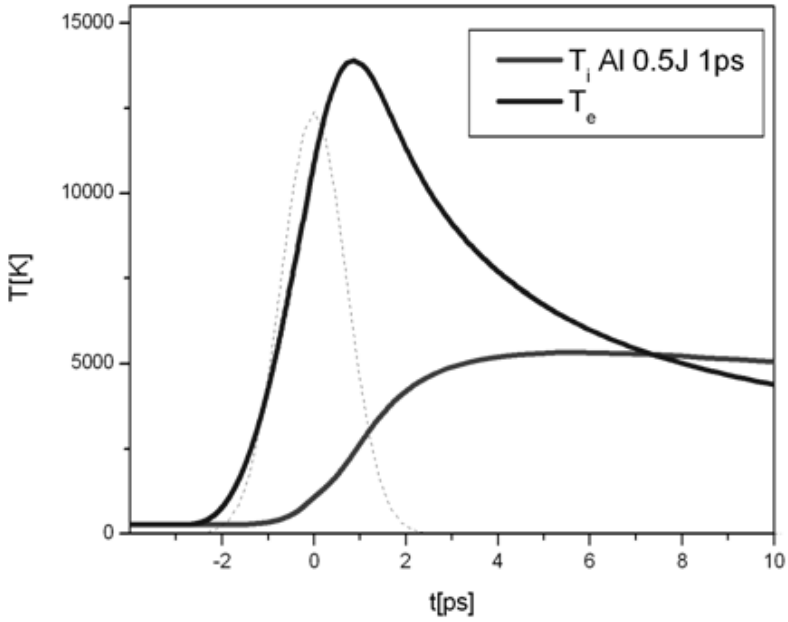

Fig. 6: Time dependence of electron and phonon temperature for $\tau = 1ps$

3.1. Nanosecond action

Due to the high value of the energy exchange coefficient $g(T_e)$, heating with a relatively long pulse in Aluminum results in a mild non-equilibrium heating. The difference between electron and phonon temperature is $\approx 150 \div 200K$, Fig.3. Melting starts at the maximum value of intensity ($t \approx 0$) and reaches the velocity of 170 m/s, Fig.4, resulting in generation of pressure in solid of the value of $\approx 3 \times 10^3$ bar. However, even relatively low melting velocity and degree of non-equilibrium of heating result in noticeable overheating of the melting surface, Fig.5 and sub-surface region of solid $\Delta T_{ph} \approx 55K$.

3.2. Picosecond action

Decrease of laser pulse duration to the value of $\tau = 1ps$ (absorbed intensity $G_0 \approx 5 \times 10^{10}$ W/cm^2) is characterized by very high rate of energy deposition. Fig.6 shows time dependence of the surface temperature $T_e(t), T_{ph}(t)$. The time profile $T_e(t)$ is noticeably shifted relative to the pulse, reaching maximum value of $T_{e\max}(t) \approx 1.3 \cdot 10^4 K$ after the time of the peak intensity ($t \approx +1ps$), Fig.6. The maximum value of the lattice temperature $T_{ph,\max} \approx 5.5 \cdot 10^4 K$ is reached at the end of the pulse. The maximum difference between electron and phonon temperature is $\Delta T = T_e - T_{ph} \approx 1.2 \times 10^4 K$. Equilibration of temperatures occurs during the time of $\approx 8ps$. High heating rate causes high rate of phases transformations. Fig. 7 shows time dependence of the melting front velocity $\upsilon_{sl}(t)$. Melting occurs at the front edge of the laser pulse and reaches its maximum value of $\upsilon_{sl\max}(t) \approx 2.75$ km/s at $t \approx +4ps$.

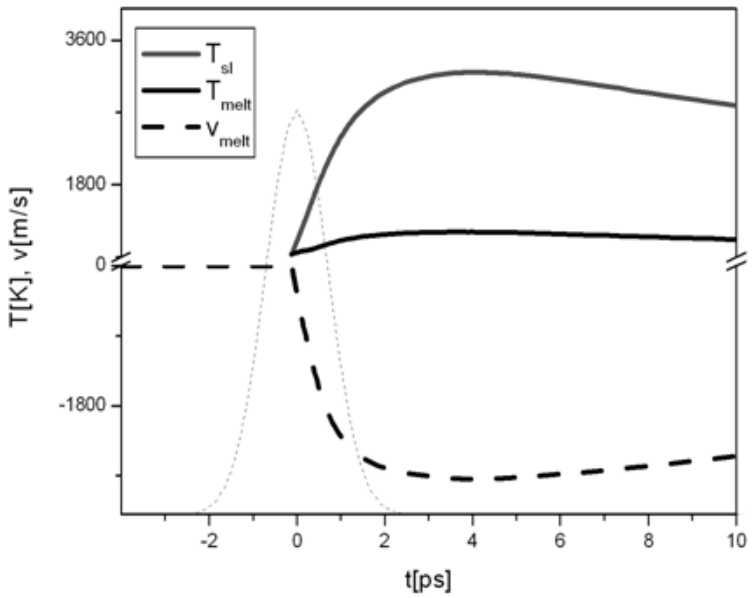

Fig. 7: Time dependence of the melting border temperature $T_{sl}(t)$, equilibrium melting temperature $T_m(P_s)$ and melting front velocity $\upsilon_{sl}(t)$ for $\tau = 1ps$

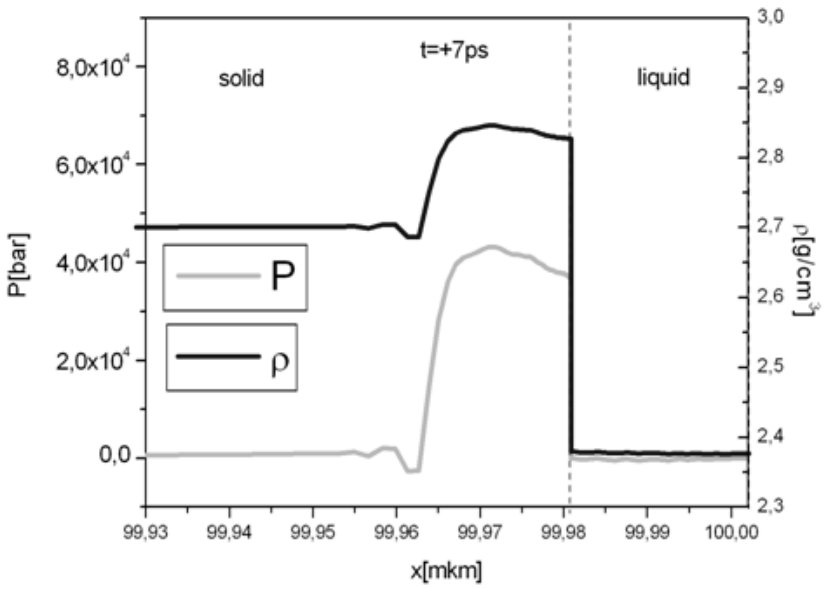

Fig.8: Spatial profiles of pressure $P_s(x)$ for $\tau = 1ps$

Such a high velocity results in a pressure build-up at the melting surface $P_s \approx 7 \times 10^4$ bar and formation of a shock wave moving in front of the melting front, Fig.8.

High velocity of the melting front is associated with strong material and energy flows through the interphase boundary. Together with the volume type of energy transfer from the electron

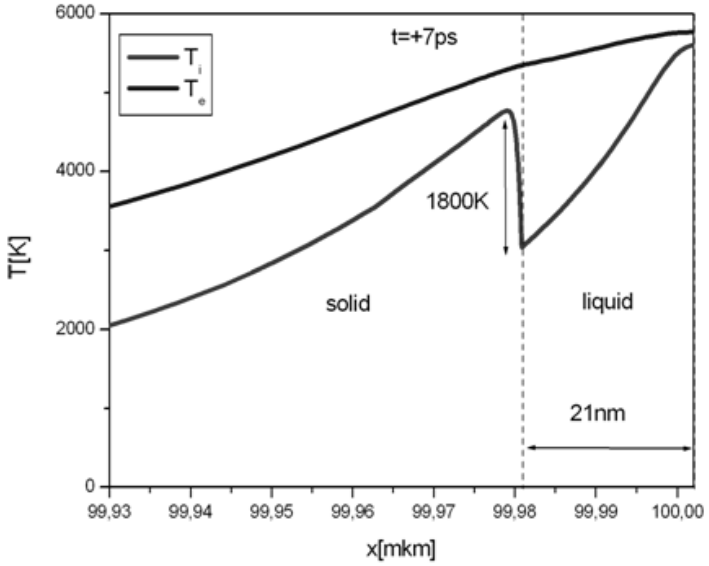

Fig. 9: Spatial profile of T_e and T_{ph} for $\tau = 1ps$

gas to the lattice, it results in the formation of highly overheated metastable region characterized by the appearance of the sub-surface temperature maximum $\Delta T_{ph} \approx 1800K$ in solid, Fig.9. The surface of solid is overheated even more, $\Delta T_{\max} = T_{sl} - T_m \approx 2000K$, Fig.7.

Thus, picosecond laser action is accompanied by the appearance the highly overheated metastable states and the fast phase transitions with velocity comparable to the one of sound.

4. Conclusion

Mathematical modeling using non-equilibrium melting model indicate the presence of an overheating of the solid phase (relative to the equilibrium melting temperature) during pulsed laser action in wide range of duration $\tau \le 10^{-9} s$. The magnitude of the overheating is in the end determined by the energy deposition rate. Its typical value for short action $\tau = 10^{-9} s$ is tens and hundreds of degrees. Ultrashort action is characterized by the generation of shock waves and metastable overheated states with the magnitude of several thousands of degrees.

Work is supported by RFFI (projects N 10-07-00246-a, N 10-07-00246-ofi-m).

5. References

1. Springer Series in Materials Science, Eds. Miotello, A.; Ossi, P.M.; Springer-Verlag Berlin Heidelberg, 201, vol. 130.
2. Lin, Zh.; Zhigilei, L.V.; Celli, V.; Phys. Rev. B., 2008, vol. 77, p. 075133-1.
3. Cheng, Ch.; Xu, X.; Phys. Rev. B., 2005, vol. 72, p. 165415-1.
4. Crout, D.; J. Math. Phys., 1936, vol. 15, p. 1.
5. Mazhukin, A.V.; Chichkov, B.N.; Book of abstracts of E-MRS 2008 Spring Meeting E-MRS, 2008, p.b-17.
6. Mazhukin, V.I.; Mazhukin, A.V.; Koroleva, O.N.; Laser Phys., 2009, vol. 19, p. 1179.